

Paleogeographic evolution of the Southern Pannonian Basin: $^{40}\text{Ar}/^{39}\text{Ar}$ age constraints on the Miocene continental series of Northern Croatia

Oleg Mandic · Arjan de Leeuw · Jeronim Bulić ·
Klaudia F. Kuiper · Wout Krijgsman ·
Zlata Jurišić-Polšak

Received: 10 November 2010 / Accepted: 2 July 2011
© Springer-Verlag 2011

Abstract The Pannonian Basin, originating during the Early Miocene, is a large extensional basin incorporated between Alpine, Carpathian and Dinaride fold-thrust belts. Back-arc extensional tectonics triggered deposition of up to 500-m-thick continental fluvio-lacustrine deposits distributed in numerous sub-basins of the Southern Pannonian Basin. Extensive andesitic and dacitic volcanism accompanied the syn-rift deposition and caused a number of pyroclastic intercalations. Here, we analyze two volcanic ash layers located at the base and top of the continental series. The lowermost ash from Mt. Kalnik yielded an $^{40}\text{Ar}/^{39}\text{Ar}$ age of 18.07 ± 0.07 Ma. This indicates that the marine-continental transition in the Slovenia-Zagorje Basin, coinciding with the onset of rifting tectonics in the Southern Pannonian Basin, occurs roughly at the Eggenburgian/Ottangian boundary of the regional Paratethys

time scale. This age proves the synchronicity of initial rifting in the Southern Pannonian Basin with the beginning of sedimentation in the Dinaride Lake System. Beside geodynamic evolution, the two regions also share a biotic evolutionary history: both belong to the same ecoregion, which we designate here as the Illyrian Bioprovince. The youngest volcanic ash level is sampled at the Glina and Karlovac sub-depressions, and both sites yield the same $^{40}\text{Ar}/^{39}\text{Ar}$ age of 15.91 ± 0.06 and 16.03 ± 0.06 Ma, respectively. This indicates that lacustrine sedimentation in the Southern Pannonian Basin continued at least until the earliest Badenian. The present results provide not only important bench marks on duration of initial synrift in the Pannonian Basin System, but also deliver substantial backbone data for paleogeographic reconstructions in Central and Southeastern Europe around the Early–Middle Miocene transition.

Electronic supplementary material The online version of this article (doi:[10.1007/s00531-011-0695-6](https://doi.org/10.1007/s00531-011-0695-6)) contains supplementary material, which is available to authorized users.

O. Mandic (✉)
Department of Geology and Paleontology, Natural History
Museum Vienna, Burgring 7, 1010 Wien, Austria
e-mail: oleg.mandic@nhm-wien.ac.at

A. de Leeuw · W. Krijgsman
Paleomagnetic Laboratory 'Fort Hoofddijk', Utrecht University,
Budapestlaan 4, 3584 CD Utrecht, The Netherlands

J. Bulić · Z. Jurišić-Polšak
Croatian Natural History Museum, Demetrova 1,
HR-10000 Zagreb, Croatia

K. F. Kuiper
Department of Isotope Geochemistry, Vrije Universiteit
Amsterdam, De Boelelaan 1085, 1081 HV Amsterdam,
The Netherlands

Keywords Ar/Ar chronology · Basin evolution ·
Pannonian Basin · Dinaride Lake System · Paratethys

Introduction

The Pannonian Basin is the largest extensional basin in a back-arc tectonic setting that formed during the Miocene in Central Europe (Fig. 1). Its evolution was strongly determined by complex intra-European plate tectonic processes of continental collision and subduction, which also generated the Alpine-Carpathian-Dinaride mountain belt (Horvath and Tari 1999; Fodor et al. 1999; Schmid et al. 2008). The Southern Pannonian Basin (SPB; Fig. 2) comprises a series of depressions with largest Sava and Drava depression attaining up to 6,000 m (Saftić et al. 2003). Their initiation started in the early-middle Miocene by continental rifting

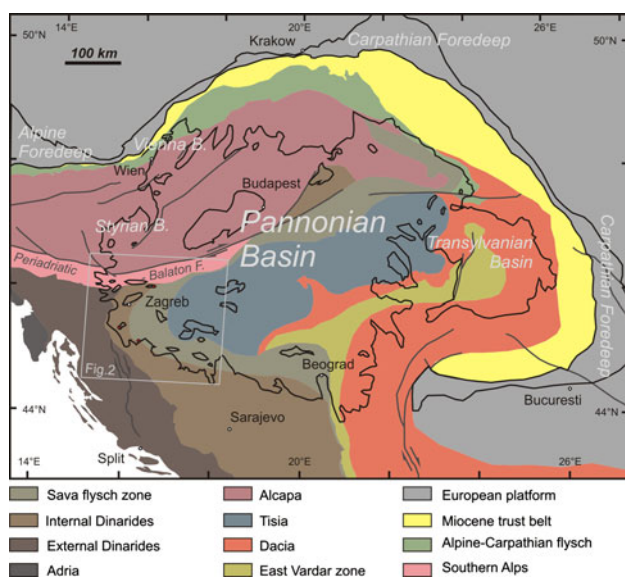


Fig. 1 Geotectonic map of the Pannonian Basin System and adjacent fold-thrust belts (modified after Schmid et al. 2008)

through lithosphere thinning along with reactivation of large, Oligocene dextral transform faults (Pavelić 2001; Hrvatović 2006). This extensional phase was accompanied by strong andesitic and rhyolitic volcanic activity (Konečný et al. 2002; Kovács et al. 2007).

Typical sedimentary successions of the initial SPB comprise continental, alluvial and lacustrine sediments unconformably overlying a strongly tectonized basement (Pavelić et al. 2003). The only exception is that stripe of the Slovenia-Zagorje Basin (SZB in Fig. 2), where an alluvial series terminates the Oligocene to Early Miocene marine deposition related to the Trans-Tethyan Trench Corridor (Rögl 1998). The superposing lacustrine series contains characteristic faunal elements of high similarity with the Dinaride Lake System to the south, thus belonging to the same bioprovince (Kochansky-Devidé and Sliškočić 1978; Bulić and Jurišić-Polšak 2009). The continental fluvo-lacustrine series is generally overlain by transgressive marine deposits representing a wide-spread ingression of the Paratethys Sea into the SPB.

Two volcanic ash-levels, one at the base and one at the top of the continental series, were sampled here for Ar/Ar dating. The lower volcanic ash helps determine the age of the initial rifting tectonics of the SPB and the marine-continental transition in the Slovenia-Zagorje Basin. The upper volcanic ash establishes the age of the lacustrine units and the maximum possible age for the initial Paratethys transgression. In combination, they provide new insights into the duration and evolution of the Dinaride Lake System (Krstić et al. 2003; Harzhauser and Mandić 2008).



Fig. 2 The map shows the position of geographic and geologic features from the southern Pannonian Basin and adjoining Dinaride-Alpine fold-thrust belts that are referred to in the text. The white-shaded area represents Miocene to Pleistocene infill of the Pannonian Basin System starting with the Middle Miocene marine flooding. The dark green-shaded areas are Lower to Middle Miocene lacustrine deposits. Compiled after Fodor et al. (1999), Tomljenović and Csontos (2001), Jelen and Rifelj (2003), Pavelić et al. (2003), Saftić et al. (2003), Placer (2008), geologic maps of former Yugoslavia M 1:100,000 and M 1:500,000 and ESRI ArcGIS base maps. SZB Oligocene to Lower Miocene Slovenia-Zagorje Basin, PB Pannonian Basin, PF Periadriatic Fault, LF Lavantal Fault, SF Šoštanj Fault, CF Celje Fault, DoF Donat Fault, LjF Ljutomer Fault, BF Balaton Fault, NF Nagykanizsa Fault, SF Sava Fault, DrF Drava Fault

Geological setting

The series of depressions that form the SPB is located at the northern part of the Dinaride mountains (Fig. 1). These mountains formed in the Eocene by thrust sheet stacking related to subduction and collision with the Tisia microplate in the north and the Adriatic microplate in the south (Pamić et al. 1998; Tari and Pamić 1998; Tari 2002; Bennet et al. 2008; Tomljenović et al. 2008; Schmid et al. 2008). The largest basins are the Sava and Drava depressions, both representing trough-like NW–SE-oriented structures, wherein the Sava and Drava rivers now flow in a southeastern direction (Fig. 2). These basins are mostly situated in Northern Croatia, but extend partly into northern Bosnia and Herzegovina (Sava depression) and southern Hungary (Drava depression). The basement belongs to the Internal Dinarides, but shows the typical NW–SE Dinaride strike direction only in southern outcrops.

The sedimentary infill of the SPB is up to 6,000 m thick and is divided into three megacycles reflecting the geodynamic history of the Pannonian Basin (Saftić et al. 2003). Our investigation deals with the lower part of the first cycle. It represents the initial syn-rift phase of the

Pannonian Basin, comprises an upward succession of alluvial/lacustrine deposits and terminates with the marine deposits of the Paratethys transgression. The Sava and Drava depressions accumulated thick clastic deposits plumbed by mud rocks that trapped significant oil accumulations from basement rocks (Lučić et al. 2001; Saftić et al. 2003; Dolton 2006). Our study areas are located at the western margin of the Drava depression (Mt. Kalnik) and at the southwestern margin of the Sava depression (Karlovac and Glina sub-depressions; Fig. 2).

Mt. Kalnik area

The inselberg Mt. Kalnik has a NE-SW strike and represents probably the rotated thorn of the westernmost Internal Dinaride extension (Fig. 1). That block was displaced during the Oligocene in a northeastern direction along the Periadriatic Fault Zone (PFZ; Tomljenović et al. 2008; Placer 2008; Fig. 1). PFZ comprises Periadriatic, Donat, Ljutomer and Balaton Faults (Fig. 2). Particularly, along the Donat Fault the Oligocene dextral displacement in order of 50 km is detected by vitrinite reflectance data (Sachsenhofer et al. 2001). During initial Pannonian Basin syn-rift in the Karpatian (latest Early Miocene), the Donat transpressive/transensional zone delineated the graben structure above the Ljutomer Fault in the southernmost Mura depression (Fodor et al. 2002; Jelen and Rifelj 2003). No Karpatian marine deposits have been ever detected south to that paleograben (Jelen and Rifelj 2003; Rasser et al. 2008).

The area of Mt. Kalnik (Fig. 2) represented during Oligocene and Early Miocene the southeastern boundary of the Slovenia-Zagorje Basin (SZB), known also as Trans-Tethyan Trench Corridor (Rögl 1998). It acted as marine connection between the Paratethys and the Mediterranean. Whereas the compression of the Adria tectonic block against the Europe resulted in SZB inversion and its subareal exposure in the Early Miocene (Jelen and Rifelj 2003), the extension due to lateral escape of the Alcapa block along the PFZ (Fig. 1) triggered consequently the formation of the Pannonian Basin (Schmid et al. 2008). Hence, the SZB-related tectonostratigraphic unit comprises paralic coal bearing, marginal marine Egerian deposits overlain by Eggenburgian shallow marine glauconitic sands (Poljak 1942; Šikić and Jović 1968; Šimunić et al. 1990; Aničić et al. 2002; Jelen and Rifelj 2003). The deposition of Egerian and Eggenburgian sediments was accompanied by strong, PFZ-related, andesitic volcanic activity (Šimunić and Pamić 1993; Altherr et al. 1995; Tibljaš et al. 2002). The subsequent Pannonian Basin tectonostratigraphic unit is marked at Mt. Kalnik with freshwater deposits transgressively overlain by the Badenian (Middle Miocene) marine sediments. It starts with fluvial siltstones, sandstones and conglomerates, passing upwards

into lacustrine marls and sandstones (Pavelić et al. 2001). Based on microfloristic evidence and on the regional stratigraphic context, the fluvial deposits are attributed to the lower Ottnangian, the lake deposits to the upper Ottnangian (Pavelić et al. 2001).

Karlovac and Glina sub-depressions

The southwestern margin of the Sava depression is marked by two sub-depressions (Karlovac and Glina) divided by the SSW-NNE striking Paleozoic and Mesozoic basement rocks of Kamešnica hill (Fig. 2). These sub-depressions are delineated in the SE by Paleozoic rocks, Jurassic ophiolites and Eocene flysch deposits (Schmid et al. 2008; Tomljenović et al. 2008). The margin in the NW is determined by Triassic platform carbonates and Cretaceous flysch. The lacustrine series, rich in mollusks (Kochansky-Devidé and Šlišković 1978 and reference therein), bears coal deposits that were exploited until the 2nd world war (Jurković 1993). According to Saftić et al. (2003), the Karlovac sub-depression comprises more than 1.5-km thick infill, the Glina sub-depression more than 0.5-km thick infill of Neogene sediments. Based on facies distribution inferred from well data, Pletikapić (1960) argued that, during lacustrine deposition, the Sava and Glina depressions were disconnected through a longitudinal ridge made up of Eocene rocks. In the Karlovac sub-depression, the basal lacustrine deposits are outcropping only at the southern part of Kamešnica hill (Fig. 2). These deposits are more common in the Glina sub-depression and can be found along its entire margin. Volcanic ash intercalations in the lacustrine sediments of Glina were described earlier by Mutić (1979). According to that author, they comprise andesitic-dacitic crystallivetroclastic and vitroclastic tuffs dominated by quartz, plagioclases and biotite.

Ar/Ar geochronology

Sections and materials

The volcanic ash at the base of the continental series was sampled at the eastern part of Mt. Kalnik, in the Glogovnica brook (GPS WGS 1984: 46.15858, 16.525669; about 20 km SE of Varaždin; Fig. 2). This is the easternmost of three localities collectively termed Knežev jarak by Tibljaš et al. (2002; pers. comm.). The tephra layer at Glogovnica brook represents a massive bed of 2-m gray, compacted, clayey biotite-bearing ash superposed by 6.7 m of a whitish to light grayish, non-consolidated, strongly altered silty ash bed. This suggests intensive volcanic activity close to the site. The section starts with 0.5-m coarse to fine-grained conglomerates overlain by 0.5-m coarse to middle-grained

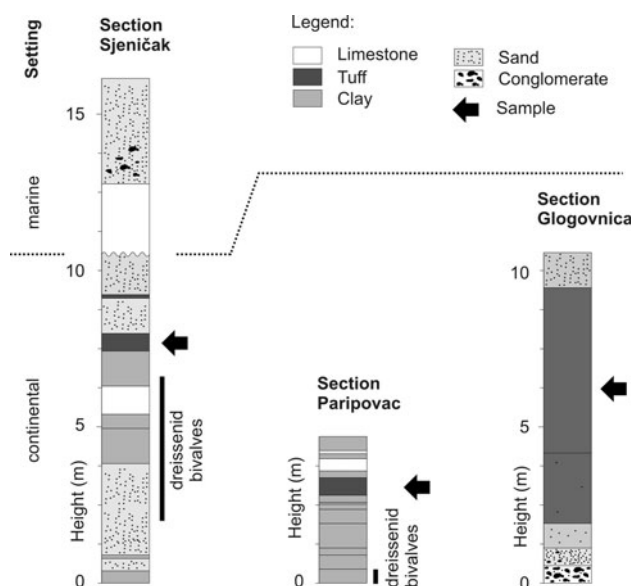


Fig. 3 Studied sections showing position of dated samples

grayish brown sandstones. This is followed, up to the ash base, by 0.7 m of sandy, micaceous clay. The ash is finally superposed by 1 m of clayey sand (Fig. 3). The sampled sedimentary succession at Mt. Kalnik lacks fossils.

The volcanic ash at the upper part of the lacustrine sediments was sampled at two localities (30 km apart) in the southern Sava depression (Fig. 2). The western locality is in the Karlovac sub-depression, close to the village Sjeničak (GPS WGS 1984: 45.422371, 15.797117). The eastern locality is in the Glina sub-depression, in the Paripovac brook north of the village Mali Gradac (GPS WGS 1984: 45.273135, 16.234022). In both localities, this volcanic ash layer is only ~ 0.5 m thick. At Sjeničak, it is represented by a biotite-bearing montmorillonite clay layer. Below the ash, more than 6 m of interbedded sands, pelites and limestone are present. They bear an accumulated lacustrine mollusk fauna dominated by *Mytilopsis* bivalves. The ash layer itself is positioned ~ 2 m below the transgression horizon, which is marked by marine organogenic limestones of Badenian age. That 2-m-thick limestone horizon is superposed finally by about 3-m-thick fining upward interval of marine conglomerate and sand. At Paripovac brook, the ash is gray medium sand with white calcite veins and biotite flakes up to 1.5 mm in diameter. It is intercalated in a thin sedimentary sequence of 2 m of clays and silts bearing accumulated *Mytilopsis* shells below the ash and about 1 m of clays and lacustrine limestone above the ash.

Methods

The bulk ash samples were crushed, disintegrated in a dilute calgon solution, washed and sieved over a set of

sieves between 63 and 500 μm and the largest appropriate mineral fraction was subjected to standard heavy liquid and magnetic separation techniques for sanidine (non-magnetic, $\delta 2.55\text{--}2.60$). All samples were subsequently hand-picked and leached with a 1:5 HF solution in an ultrasonic bath for 5 min.

The resulting mineral separates were then sent for irradiation at the Oregon State University TRIGA reactor in the cadmium-shielded CLICIT facility for 10 h. Upon return to the VU Argon Laboratory, the samples were pre-heated under vacuum using a heating stage and heat lamp to remove undesirable atmospheric argon. Thereafter, samples were placed in an ultra high vacuum sample chamber and degassed overnight. For each ash sample, 10 multiple-grain splits of the mineral separate were fused using a Synrad CO₂ laser in combination with a Raylase scanhead as a beam delivery and beam diffuser system. After purification, the resulting gas was analyzed with a Mass Analyzer Products LTD 215-50 noble gas mass spectrometer. Beam intensities were measured in a peak-jumping mode in 0.5 mass intervals over the mass range 40–35.5 on a Balzers 217 secondary electron multiplier. System blanks were measured every three to four steps. Mass discrimination was monitored by frequent analysis of aliquots of air. The irradiation parameter J for each unknown was determined by interpolation using a second-order polynomial fitting between the individually measured standards.

All $^{40}\text{Ar}/^{39}\text{Ar}$ ages have been calculated with the ArArCalc software (Koppers 2002), applying the decay constants of Steiger and Jäger (1977). The age for the Fish Canyon Tuff sanidine flux monitor used in age calculations is 28.201 ± 0.03 Ma (Kuiper et al. 2008). The age for the Drachenfels sanidine flux monitor is 25.477 ± 0.03 Ma (see Appendix). Correction factors for neutron interference reactions are $2.64 \pm 0.017 \times 10^{-4}$ for $(^{36}\text{Ar}/^{37}\text{Ar})_{\text{Ca}}$, $6.73 \pm 0.037 \times 10^{-4}$ for $(^{39}\text{Ar}/^{37}\text{Ar})_{\text{Ca}}$, $1.211 \pm 0.003 \times 10^{-2}$ for $(^{38}\text{Ar}/^{39}\text{Ar})_{\text{K}}$ and $8.6 \pm 0.7 \times 10^{-4}$ for $(^{40}\text{Ar}/^{39}\text{Ar})_{\text{K}}$. Errors are quoted at the 1σ level and include the analytical error and the error in J .

Results

An overview of the results is displayed in Table 1. All relevant analytical data as well as error determination are presented in Table 2a–c and in the online supplementary material. For each of the Glogovnica, Sjeničak and Paripovac ashes, 10 multiple-grain single-fusion experiments were performed (Table 2). Mass discrimination was monitored frequently during the analytical runs and was not always stable. We ignored all data with unlikely high (>1.0150) mass discrimination corrections. The uncertainty

Table 1 Summary of the $^{40}\text{Ar}/^{39}\text{Ar}$ results

Sample	Location	Weighted mean age (Ma)	<i>n</i>	<i>N</i>	MSWD	Mineral	Inverse isochron age	Isochron intercept
Glogovnica	N46.158580 E016.525669	18.07 ± 0.07	5	10	1.26	Sanidine	18.04 ± 0.07	360 ± 38
Sjeniĉak	N45.422371 E015.797117	15.91 ± 0.06	5	10	1.18	Sanidine	15.89 ± 0.06	303 ± 6
Paripovac	N45.273135 E016.234022	16.03 ± 0.06	6	9	2.04	Feldspar	16.04 ± 0.06	295 ± 5

MSWD mean square weighted deviates, *n* is the number of experiments used to calculate the weighted mean and isochron age, *N* is the total number of repetitions in the single-fusion experiments

in our discrimination correction is therefore ~0.2–0.3% depending on the stability of air measurements run before and after our unknowns.

For the Glogovnica ash, 5 out of 10 experiments were selected to calculate the weighted mean age of 18.07 ± 0.07 Ma (Fig. 4; Table 2a), with the mean square weighted deviates (MSWD) of 1.26 and with an isochron age of the 18.04 ± 0.07 Ma (Table 1). Experiments 48A and B were discarded based on their high mass discrimination correction indicating peak calibration problems of the mass spectrometer. After magnet calibrations, the experiment was continued. Experiments 48I and M were excluded due to their comparatively low K/Ca content, indicating the presence of a lower K mineral. Experiment 48H was discarded because the mass spectrometer encountered peak centering problems during this experiment. The error in the isochron intercept for the Glogovnica experiments is large due to the high percentage of radiogenic argon and resultant clustering of data points.

A weighted mean age of 15.91 ± 0.06 Ma was calculated based on 5 out of the 10 experiments performed for the Sjeniĉak ash (Fig. 4, Table 2b). The weighted mean age is concordant with the 15.89 ± 0.06 Ma isochron age (MSWD = 1.91) (Table 1). Experiment 50G and 50K were discarded because they are significantly younger than other experiments. Experiments 50H, 50L and 50A were identified as outliers by comparing MSWD with the *T*-student distributions at the 95% significance level (Koppers 2002).

The weighted mean age of 16.03 ± 0.06 Ma for the Paripovac ash was calculated based on 6 out of the 9 measured experiments (Fig. 4; Table 2c). The weighted mean age is concordant with the 16.04 ± 0.06 Ma isochron age (MSWD = 2.04) (Table 1). The mass discrimination factor was more stable during the measurement of the Paripovac experiments and none had to be discarded on these grounds. Experiments 59A and F were excluded when calculating the weighted mean age because they are significantly younger than the other experiments. Experiment 59L was discarded because problems with peak centering were encountered during measurement.

For all three ash samples, outliers were further identified until the MSWD of the calculated weighted mean ages was

smaller than the *T*-student distribution at the 95% confidence level (Table 2a–c). The weighted mean ages were concordant with the isochron ages and very close to the main peak in probability density distribution, even though the age populations in the latter were not completely homogeneous. We therefore interpret them to reflect the tuffs' crystallization ages. The ages for the Paripovac and Sjeniĉak ashes are in excellent agreement and suggest that we are dealing with the same volcanic event, even though the great difference in their K/Ca ratio indicates that we separated and dated a material with a different chemical composition.

Discussion

Initiation of extensional tectonics in the South Pannonian Basin

The volcanic ash from the Glogovnica tuff at Mt. Kalnik is stratigraphically located in the basal part of the fluvial-lacustrine deposits of the Drava depression. Following to inversion of the Oligocene-Lower Miocene Slovenia-Zagorje Basin (Paveliĉ et al. 2001; Jelen and Rifelj 2003; Fig. 2), this new tectonostratigraphic cycle reflects the beginning subsidence in the Pannonian Basin. The new Ar/Ar dating of the Glogovnica tuff indicates that this initial rifting phase of the SPB took place at 18.07 ± 0.07 Ma (Figs. 4 and 5). This corresponds stratigraphically roughly to the Eggenburgian/Ottangian transition in the Paratethys time scale (Piller et al. 2007) and to the middle Burdigalian of the standard Geological Time Scale (Lourens et al. 2004). The Eggenburgian/Ottangian transition corresponds to a major global sea-level low-stand event marking the third-order sequence boundary Bur-3 (Piller et al. 2007).

The sedimentary successions of the continental basinal infill of the various SPB depressions generally show a similar architecture, with alluvial sediments in the lower part and lacustrine sediments in the upper part (Paveliĉ 2001). Such an architecture is present everywhere along the basinal margins, e.g., in the region of Mt. Źumberak (Vrsaljko et al. 2005), Mt. Medvednica (Paveliĉ et al.

Table 2 Most relevant analytical data for the dated Glogovnica (a), Sjeničak (b) and Paripovac (c) ashes

(a)										
Total laser fusion	36Ar(a)	37Ar(ca)	38Ar(cl)	39Ar(k)	40Ar(r)	Age $\pm 2\sigma$ (Ma)	40Ar(r) (%)	39Ar(k) (%)	K/Ca $\pm 2\sigma$	
08 MX048A	7.00 W	0.000890	0.025569	0.000000	3.854476	17.46 \pm 0.08	98.11	13.54	64.8 \pm 8.2	
08MX048B	7.00 W	0.000382	0.019544	0.000000	3.101401	17.52 \pm 0.08	98.98	10.90	68.2 \pm 10.4	
08MX048P	7.00 W	x	0.000136	0.000000	3.408423	18.00 \pm 0.11	99.66	11.98	68.2 \pm 9.0	
08MX048Q	7.00 W	x	0.000116	0.025665	3.309941	18.03 \pm 0.11	99.70	11.63	55.5 \pm 7.4	
08MX048 N	7.00 W	x	0.000216	0.020100	2.896707	18.07 \pm 0.12	99.39	10.18	62.0 \pm 9.6	
08MX048L	7.00 W	x	0.000176	0.022689	3.107143	18.11 \pm 0.11	99.53	10.92	58.9 \pm 6.7	
08MX048 J	7.00 W	x	0.001039	0.018700	2.930700	18.14 \pm 0.12	97.25	10.30	67.4 \pm 8.9	
08 MX048M	7.00 W	x	0.000429	0.125977	1.919224	18.20 \pm 0.12	98.24	6.74	6.6 \pm 0.2	
08MX048H	7.00 W	x	0.000280	0.018980	2.767688	18.22 \pm 0.12	99.19	9.72	62.7 \pm 15.5	
08MX048I	7.00 W	x	0.000330	0.535383	1.163888	18.41 \pm 0.14	97.82	4.09	0.9 \pm 0.0	
		Σ	0.003994	0.834102	28.459590	105.180187				
(b)										
Information on analysis	Results	40(r)/39(k) $\pm 2\sigma$	MSWD	39Ar(k) (%)	n	K/Ca $\pm 2\sigma$				
Sample = VU69-A14	Age plateau	3.7178	0.92	55.00	5	61.4 \pm 4.9				
Material = sanidine		± 0.0106								
Location = Glogovnica		$\pm 0.29\%$								
Analyst = Arjan de Leeuw			2.78	Statistical T ratio						
Project = VU69			1.0000	Error magnification						
Mass discrimination law = LIN	Total fusion age	3.6958		10		14.7 \pm 0.3				
Irradiation = VU69		± 0.0072								
J = 0.00270786 \pm 0.00000812		$\pm 0.20\%$								
Dra-1 = 25.477 \pm 0.031 Ma (this study)										
(b)										
Total laser fusion	36Ar(a)	37Ar(ca)	38Ar(cl)	39Ar(k)	40Ar(r)	Age $\pm 2\sigma$ (Ma)	40Ar(r) (%)	39Ar(k) (%)	K/Ca $\pm 2\sigma$	
08MX050 K	7.00 W	0.001310	0.031148	0.000000	4.648759	15.69 \pm 0.08	97.48	11.24	64 \pm 9	
08MX050G	7.00 W	0.003025	0.024890	0.001102	3.974565	15.71 \pm 0.09	93.52	9.61	69 \pm 8	
08MX050P	7.00 W	x	0.004706	0.000493	4.650596	15.87 \pm 0.09	91.65	11.24	62 \pm 5	
08MX050O	7.00 W	x	0.001027	0.029889	4.326528	15.87 \pm 0.08	97.89	10.46	62 \pm 8	
08MX050I	7.00 W	x	0.002229	0.026540	4.207589	15.91 \pm 0.09	95.45	10.17	68 \pm 9	
08MX050Q	7.00 W	x	0.008975	0.027826	3.901584	15.92 \pm 0.11	82.92	9.43	60 \pm 8	
08MX050 M	7.00 W	x	0.006856	0.026497	4.136136	16.00 \pm 0.10	87.12	10.00	67 \pm 4	
08MX050H	7.00 W	x	0.001790	0.028195	4.339535	16.08 \pm 0.09	96.45	10.49	66 \pm 7	
08MX050L	7.00 W	x	0.006471	0.018885	2.800036	16.08 \pm 0.11	83.00	6.77	64 \pm 9	
08MX050A	7.00 W	x	0.001574	0.030498	4.374072	16.10 \pm 0.09	96.89	10.58	62 \pm 6	

Table 2 continued

Total laser fusion		36Ar(a)	37Ar(ca)	38Ar(cl)	39Ar(k)	40Ar(r)	Age ± 2σ (Ma)	40Ar(r) (%)	39Ar(k) (%)	K/Ca ± 2σ
Σ	0.037964	0.276806	0.001955	41.359400	136.628528					
Information on analysis										
Sample = VU69-A14	Results									
Material = sanidine	Age plateau	3.3014	± 0.0095	15.91	1.18	51.31	MSWD	39Ar(k) (%)	n	K/Ca ± 2σ
Location = Glogovnica			± 0.29%						5	64 ± 3
Analyst = Arjan de Leeuw	Minimal external error ± 0.12				2.78			Statistical T ratio		
Project = VU69	Analytical error ± 0.05				1.0840			Error magnification		
Mass discrimination law = LIN	Total fusion age	3.3034	± 0.0061	15.92		10				64 ± 2
Irradiation = VU69			± 0.19%							
J = 0.00268230 ± 0.00000805	Minimal external error									
Drα-1 = 25.477 ± 0.031 Ma (this study)	Analytical error									
(c)										
Total laser fusion		36Ar(a)	37Ar(ca)	38Ar(cl)	39Ar(k)	40Ar(r)	Age ± 2σ (Ma)	40Ar(r) (%)	39Ar(k) (%)	K/Ca ± 2σ
08MX059A	7.00 W	0.000468	0.191630	0.000110	3.404577	11.309923	15.63 ± 0.07	98.77	11.27	7.64 ± 0.26
08MX059F	7.00 W	0.002571	0.390555	0.000227	3.194448	10.634155	15.67 ± 0.07	93.31	10.57	3.52 ± 0.09
08MX059 K	7.00 W	0.002651	0.358426	0.000515	3.051087	10.237378	15.79 ± 0.08	92.87	10.10	3.66 ± 0.09
08MX059E	7.00 W	0.002694	0.554381	0.000604	3.656741	12.382415	15.93 ± 0.07	93.94	12.11	2.84 ± 0.06
08MX059D	7.00 W	0.018674	0.412727	0.000543	3.155372	10.742603	16.02 ± 0.16	66.05	10.45	3.29 ± 0.07
08MX059I	7.00 W	0.000816	0.478675	0.000150	3.104202	10.573596	16.03 ± 0.07	97.75	10.28	2.79 ± 0.05
08MX059B	7.00 W	0.001351	0.254108	0.000000	2.995728	10.230888	16.07 ± 0.07	96.22	9.92	5.07 ± 0.12
08MX059L	7.00 W	0.000511	0.169103	0.000201	3.818141	13.040173	16.07 ± 0.07	98.83	12.64	9.71 ± 0.34
08MX059G	7.00 W	0.008214	0.235674	0.000181	3.827499	13.073551	16.07 ± 0.09	84.32	12.67	6.98 ± 0.19
Σ	0.037950	3.045279	0.002531	30.207795	102.224684					
Information on analysis										
Results										
Sample = VU69-A14	Age ± 2σ (Ma)									
Material = sanidine	Age plateau	3.4076	± 0.0099	16.03	2.04	68.05	MSWD	39Ar(k) (%)	n	K/Ca ± 2σ
Location = Glogovnica			± 0.29%						6	3.28 ± 0.99
Analyst = Arjan de Leeuw	Minimal external error ± 0.12				2.57			Statistical T ratio		
Project = VU69	Analytical error ± 0.05				1.4280			Error magnification		
Mass discrimination law = LIN	Total fusion age	3.3840	± 0.0063	15.92		9				4.27 ± 0.03
Irradiation = VU69			± 0.18%							
J = 0.00261997 ± 0.00000786	Minimal external error									
Drα-1 = 25.477 ± 0.031 Ma (this study)	Analytical error									

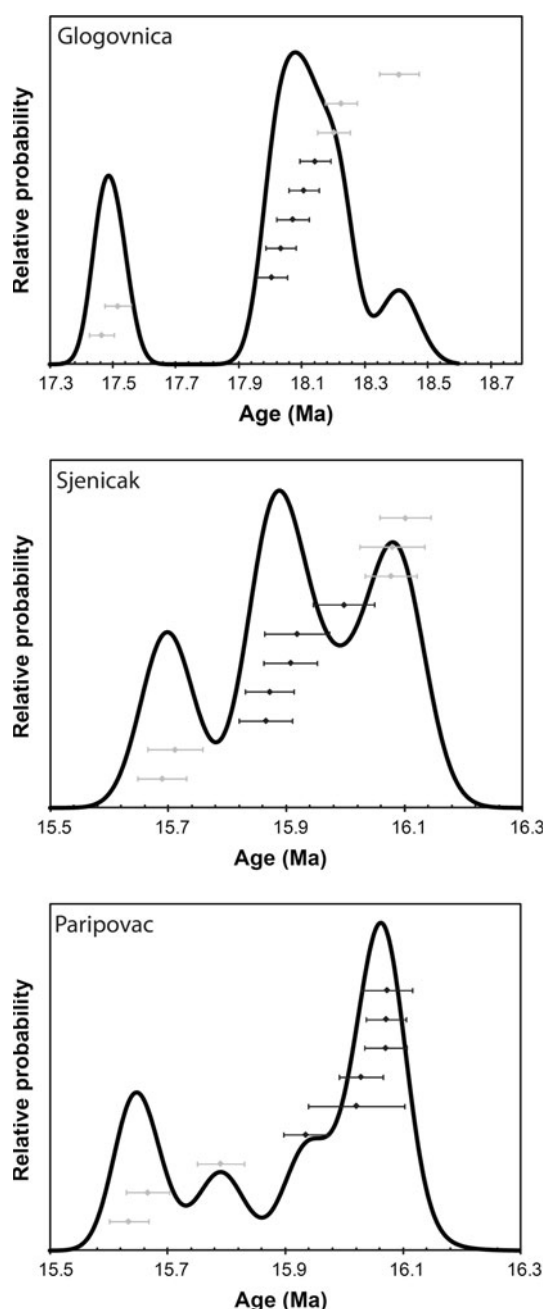


Fig. 4 Probability plots. Error bars are 1 sigma analytical errors. Black data are included in weighted mean age, gray data are excluded, see text for explanation

2001), Mt. Papuk (Pavelić et al. 1998), Mt. Požeška (Hajek-Tadesse et al. 2009) and Mt. Kalnik (Pavelić et al. 2001). Consequently, Pavelić et al. (1998) suggested a uniform opening of these basins due to tectonic rifting. According to that model, the early rifting was accompanied in the SPB by the extension of vast floodplain environments. The initial leveling of the relief was characterized by the extended accumulation of conglomerates and other fluvial material infilling the depressions. During a later

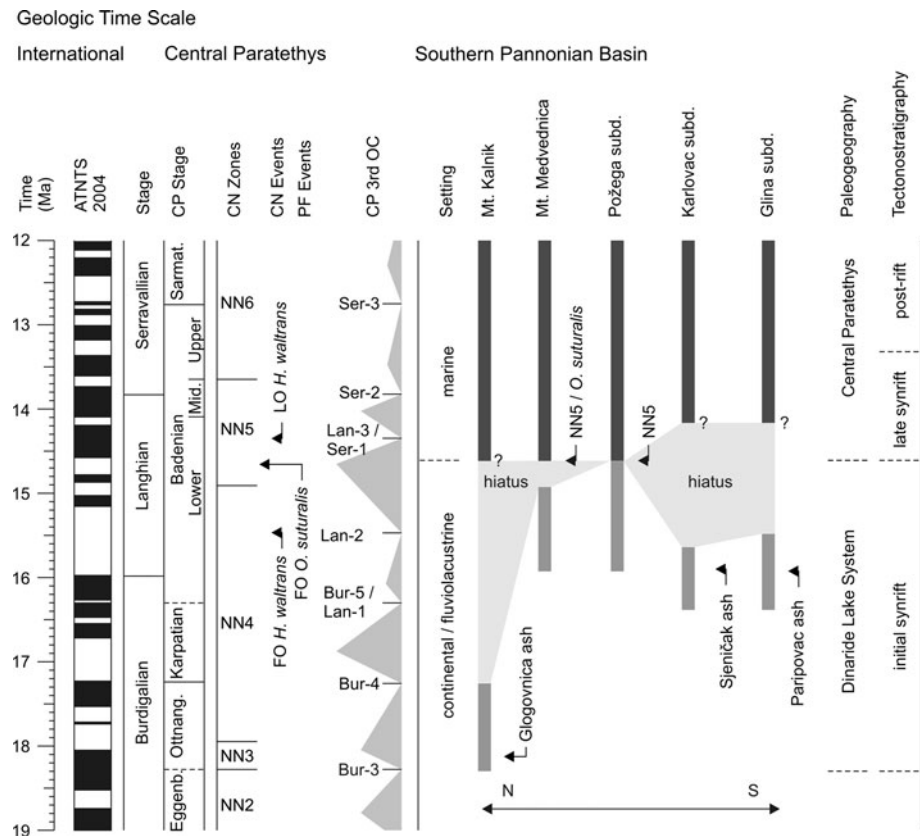
phase, larger and smaller lakes developed here. This lake development was probably an effect of more humid climate conditions following the onset of the Miocene climate optimum (Zachos et al. 2001) coinciding with increased subsidence rates in the area which promoted together lake settlement throughout the region.

In addition, the new age for the extensional tectonics of the SPB correlates exactly with the age of the initial extension and deposition in the intra-mountainous basins of the Dinaride Lake System dated currently in the Sinj Basin (De Leeuw et al. 2010). The vast area of that system, stretching southwards across the Dinarides into the Outer Dinaride Foreland Basin on the Adriatic microplate, demonstrates the extended spatial range of Pannonian Basin extensional tectonics (De Leeuw et al. 2010). The initiation of Lake Sinj in southern Croatia was recently determined by Ar/Ar dating in combination with magneto-biostratigraphic correlations to have occurred at ~ 18 Ma (De Leeuw et al. 2010). This synchronicity indicates that large-scale geodynamic processes in the Dinaride fold-thrust belt and the Pannonian region were responsible for the initial extension phase in the SPB.

Our new age constraint for the marine-continental transition fits very well with the previous age data on the basal units of the SPB. Such age is also in good agreement with the K/Ar age of 19.21 ± 0.64 Ma for the glauconite sands of the underlying marine Macelj formation (Avanić et al. 2005), which correlates to the Eggenburgian. The superposing continental series of Mt. Kalnik correlates to the Ottnangian based on pollen data (Pavelić et al. 2001). In particular, their lacustrine part corresponds to the late Ottnangian microfloristic zone MF-4 indicating the last cold spell before the start of the global warming event in the Karpatian. The subsequent thermophilous floral assemblage is known from the similar environmental setting of Mt. Moslavačka Gora at the northern margin of the Sava Depression (Krizmanić 1995). The calculated age from Mt. Kalnik is also in accordance with Tibljaš et al. (2002), who suggested that the Glogovnica ash correlates, based on its chemical composition, with Egerian and Eggenburgian andesites and dacites. Its dating with the Eggenburgian/Ottnangian boundary interval places it to the very final phase of the andesite-dacite volcanism supporting the authors' suggestion that a major change in geochemical composition of regionally very common volcanic and volcanoclastic rocks must have taken place during the Ottnangian.

In the North Hungarian Basin, positioned in NE prolongation of the Slovenia-Zagorje Basin, the corresponding continental fluvio-lacustrine series superposes marine deposits with *Pecten hornensis* of early Ottnangian age (Csepregyhyné Meznerics 1967; Piller et al. 2007). The Lower Rhyolite Tuff, intercalated in the lower part of that

Fig. 5 Geochronologic correlation table compiled after Lourens et al. (2004), Strauss et al. (2006), Piller et al. (2007), Hohenegger et al. (2009) and Ćorić et al. (2009) showing approximate depositional durations for different regions within the PBS and stratigraphic position for investigated samples. *CP* Central Paratethys, *CN* Calcareous Nannoplankton, *PF* Planktonic Foraminifera, *FO* First Occurrence, *LO* Last Occurrence, *OC* Order Cycles



continental series, was dated by the $^{40}\text{Ar}/^{39}\text{Ar}$ technique at 17.02 ± 0.14 Ma and 16.99 ± 0.16 Ma (Palfy et al. 2007). This suggests a distinctly younger, early Karpatian age for the volcanism.

Paleogeographic changes and faunal bioprovinces

The marine Egerian and Eggenburgian deposits of the Slovenia-Zagorje Basin indicate that this region formed prior to SPB installation at the southeastern margin of the Paratethys Basin (Fig. 2). During Egerian, it belonged to the Transtethyan corridor that connected the Paratethys with the Mediterranean-Tethys Sea in northeastern Italy via the North Hungarian Basin (Rögl and Steininger 1983; Rögl 1998). Our results indicate that marine environments of the Slovenia-Zagorje Basin preceding the SPB extension disappeared at 18.1 Ma during the earliest Oltngian. This involved a combination of tectonic activity and glacio-eustatic sea-level lowering.

The Oltngian and Karpatian sediments of the Paratethys region are characterized by the occurrence of brackish marine *Rzehakia* assemblages. They are considered to mark a major endemic event that can be traced all across the Paratethys Sea from Bavaria into the Caucasus (Mandic and Ćorić 2007). During this event, the entire Paratethys Sea is considered to be a separate ecoregion termed Danubian

Province (Harzhauser and Piller 2007 and references therein). The absence of *Rzehakia* shell accumulations in the entire SPB including Styrian basin, SW Hungary (up to Varpalota), and Mura, Drava and Sava depressions indicates that their connection to the Paratethys was completely lost at that time. Moreover, it shows that no Paratethys ingressions occurred in the SPB during the late Oltngian and early Karpatian: such an ingressions would have certainly brought this peculiar brackish fauna into the lake system.

The Karpatian transgression (Rögl 1998) from the Mediterranean via the Venetian and Styrian basins into the North Hungarian Basin apparently did not cross the Donat fault into the Drava and Sava depressions (Figs. 2 and 6). This transgression must have taken place at a time when *Rzehakia* was already extinct in the Paratethys because that taxon did not migrate southwards following the re-establishment of marine conditions. An absence of Karpatian marine deposits south of the Donat fault was also suggested by Rasser et al. (2008).

The biostratigraphic data from the SPB (*Mytilopsis*/dreissenid bivalves) indicate that its freshwater environments are closely related to the Dinaride Lake System that originated at the same time (Mandic et al. 2009; De Leeuw et al. 2010). The southern margin of the Sava depression shows particularly high faunal similarity with the mollusk fauna of the Dinaride intra-mountainous basins (Kochansky-Devide



Fig. 6 Paleogeographic map showing extensions of the Dinaride Lake System, Lake Serbia and the Paratethys during the Early/Middle Miocene transition (compiled after Rögl and Steininger 1983; Hámor 1988; Krstić et al. 2003, and own data). Dashed lines mark the maximal possible extension of the Illyrian Bioprovince. The geographic area is same as in Fig. 1

and Slišković 1978). Based on the high-grade endemic character (Harzhauser and Mandić 2008), these faunas are regarded to constitute an independent paleobiogeographic unit that we now term the Illyrian Bioprovince. The extension of the Illyrian Bioprovince did not always exactly correlate with the extension of the Dinaride Lake System. Especially during the Karpatian-Badenian, dreissenid-rich accumulations of the Illyrian Bioprovince extended further north to Mt. Meszesk (Hamor 1970) and Mt. Bakony (Kókay 2006) in S Hungary, to Fohnsdorf (Hölzel and Wagreich 2004) and into the Vienna Basin (Schultz 2003) in E Austria and further south to the region SSE of Belgrade (Knežević 1996) belonging to the Lake Serbia (Krstić et al. 2003) (Fig. 6).

The lacustrine deposits from the Karlovac and Glina sub-depressions are also characterized by abundant dreissenid bivalve accumulations of the Illyrian Bioprovince type, whereas these accumulations are absent in the older deposits at Mt. Kalnik. Drill holes in the Sava depression indicate that the dreissenid assemblages are restricted to the upper part of the lacustrine interval (Ožegović 1944). The volcanic ashes of Sjeniĉak and Paripovac are located at the upper part of the terrestrial series and consequently provide the youngest age for the lake deposits and the Illyrian Bioprovince in the SPB. The new Ar/Ar dating of 15.91 ± 0.06 Ma and 16.03 ± 0.06 Ma for the dreissenid assemblages for the first time prove that lacustrine sedimentation continued in the SPB at least until the earliest Badenian. This is significantly younger than the previously inferred late Otnangian age (Kochansky-Devide and Slišković 1978; Bulić and Jurišić-Polšak 2009; Hajek-Tadesse et al. 2009).

The typical sedimentary successions of the terrestrial series of the SPB show alluvial sediments in the lower part and lacustrine sediments in the upper part (Pavelić 2001). Pavelić et al. (1998) inferred a synchronous installation of a huge open lake environment, connecting all depressions of the SPB. This model was based on sections from the Požega sub-depression where marine transgression indeed flooded one deep, open lake, changing the water chemistry and introducing marine immigrants without changing the depositional facies (Pavelić et al. 1998; Hajek-Tadesse et al. 2009). In contrast, Saftić et al. (2003) claimed, based on results from the Sava and Drava depressions, that the lakes were not connected but formed rather isolated occurrences across the southern Pannonian Basin. The calculated ages of the two tephra layers together with previously discussed faunal difference suggest that the continental fluvio-lacustrine deposition is possibly not coeval across the SPB (Fig. 5). Such sedimentation occurred already in the early Otnangian at Mt. Kalnik and during the early Badenian in the southern Sava depression. These significant age differences partly fit tectonostratigraphic models for the early rifting phase of the SPB (Prelogović 1975; Pavelić 2001). These models imply an earlier development of the Drava versus the Sava depression. Accordingly, subsidence and lake development could have first started in the Drava depression, progressing later in southward direction over the Bjelovar and Požega sub-depressions to finally reach the Sava depression and its southern sub-depressions.

The Badenian transgression in the Southern Pannonian Basin

The marine Badenian transgression and opening to the world oceans represented a crucial phase in the Pannonian Basin formation, especially in the Interior Dinaride Foreland where terrestrial environments persisted since the Eocene time (Rögl 1998; Popov et al. 2004). The Sjeniĉak and Paripovac ashes are both located slightly below the marine transgression (Fig. 3), and the equivalent $^{40}\text{Ar}/^{39}\text{Ar}$ ages of ~ 16.0 Ma thus indicate the maximum age of the Badenian transgression in the SPB. This transgression is, however, biostratigraphically dated to an age younger than 14.8 Ma based on nannofossil assemblages corresponding to NN5 at Mt. Medvednica and at Mt. Papuk by Ćorić et al. (2009).

Accepting a maximum age of 14.8 Ma for the Badenian transgression at Karlovac implies a significant hiatus/interruption of sedimentation between the lacustrine deposits and the marine flooding. This discordance is also recorded at the northern margin of the sub-basin, where Badenian marine deposits directly transgress the basement rocks (Pletiković 1960). A similar conclusion must be

made for the Glina sub-depression where, according to regional stratigraphic data, the studied ash layer is overlain by coal deposits (Jurković 1993; field observation). Apparently, a swamp-related marginal lake environment installed itself, marking the final phase in regional lacustrine deposition. Similarly, very thick coal deposits can be traced in their southeastern continuation (Fig. 2), e.g., in the Lješljane Basin north of Prijedor in Bosnia and Herzegovina or in the Banja Luka Basin (Milojević 1976). The Karlovac and Glina sub-depressions could thus represent a zone independent from the Sava depression and related to the intra-mountainous basins of the Dinaride Lake System (Fig. 2). This suggests that, in contrast to Lake Požega (Požega sub-depression) in the Slavonian Mountains (Pavelić et al. 1998; Ćorić et al. 2009, Hajek-Tadesse et al. 2009), the lakes of the Karlovac and Glina sub-depressions were not directly flooded by the Middle Miocene marine water, but vanished before the transgression.

Alternatively, it is possible that the marine transgression was not coeval for the entire SPB. This would diminish the significance of the latter result. In particular, the biostratigraphic data available from the region NE of Banja Luka and Prijedor in Bosnia and Herzegovina suggest that the marine transgression first reached the southern sub-depressions of the Sava Depression in the late Early Badenian (Petrović and Atanacković 1969, 1976; Fig. 5). Future investigations of the Drava Depression should focus on demonstrating the age of its initial marine flooding in respect to the previously reported Karpatian datum (Pavelić et al. 2001). Within the Hungarian part of that depression, the marine transgression is attributed to the Badenian (Saftić et al. 2003). Data from Slovenia fix the position of the southernmost Karpatian deposits at the Donat fault (Rasser et al. 2008), striking along the northwestern boundary of the Drava depression (Fig. 2). At Mt. Vilanny north of the Drava depression, the marine flooding is also settled into the Badenian (Saftić et al. 2003). There, the lake deposits underlying the transgression bear common dreissenid shell accumulations (Hamor 1970), suggesting its relation to the younger part of the SPB basal fluvio-lacustrine infill.

Conclusions

The volcanic ash from Mt. Kalnik is dated at ~18.1 Ma and corresponds to the middle Burdigalian and the Eggenburgian-Ottangian transition. Its stratigraphic position at the base of the initial fluvial-lacustrine deposits of the Drava depression corresponds with the start of extensional tectonics in the Pannonian Basin System. Our new age correlates exactly with the age of the initial deposition in the intra-mountainous basins of the Dinaride Lake System.

This provides evidence for similar large-scale geodynamic processes in the Miocene of the Dinaride fold-thrust belt and the Pannonian Basin.

The volcanic ashes from the Karlovac and Glina sub-depressions are dated at ~16.0 Ma, corresponding to the earliest Langhian and earliest Badenian, respectively. This implies that the duration of the SPB extensional phase, characterized by fluvial and lacustrine deposition, lasted more than 2 Myr. Taking into account the revised datum of initial marine flooding in the Southern Pannonian Basin (Ćorić et al. 2009) that duration may even be extended by an additional 1 Myr.

Such a long duration of the continental cycle—in combination with available sedimentation data, sequence stratigraphy, and the position and character of marine transgression—makes continuous basin deepening models improbable. We here suggest a phase of several independent, smaller and larger basins comparable with the Dinaride intra-mountainous basins and argue that the entire study area paleogeographically and tectonically corresponds to the Dinaride Lake System and Dinaride Basins, respectively, prior to Paratethys flooding and finalization of the SPB as tectonic unit (Figs. 5 and 6).

We consider the term Paratethys exclusively related to a marine and marginal marine ecozone restricted at that time to the adjoining area north of the Donat line (Fig. 2). The endemic mollusk fauna of the basal SPB infill is similar to that of the Dinaride intra-montane basins and is attributed to the Illyrian Bioprovince, an ecoregion which is the continental counterpart to the marine Danubian Province (Harzhauser and Piller 2007) of the Paratethys domain.

Dreissenid shell accumulations with a faunal composition related to the fossil fauna of the Illyrian Bioprovince are abundantly present in sections from the Karlovac and Glina sub-depressions and are now dated to be of earliest Badenian age. These accumulations are restricted to the upper parts of the basal lacustrine deposits of the Southern Pannonian Basin. The presence of related dreissenid shell beds as far as the Vienna Basin (E Austria), Mt. Bakony (central Hungary), Mt. Mesecek (south Hungary) or the Morava Valley SSE of Belgrade (central Serbia) suggests the strikingly wide extension of the Illyrian Bioprovince during the Early and Middle Miocene.

Acknowledgments Thanks go to Jakov Radovčić (Croatian Natural History Museum, Zagreb) for help with the field work. We are highly obliged to Davor Pavelić (Faculty of Mining, Geology and Petroleum Engineering, University of Zagreb) and Mathias Harzhauser (Natural History Museum Vienna) for comments and suggestions regarding an earlier version of the manuscript. We thank Werner E. Piller (University of Graz) and Reinhard F. Sachsenhofer (University of Leoben) for reviews and valuable suggestions improving the quality of the paper. The study contributes the Austrian Science Fund (FWF) Project P18519-B17: “Mollusk Evolution of the Neogene Dinaride Lake System” and was supported by Dutch Centre for Integrated Solid

Earth (ISES) as well as Netherlands Organisation for Scientific Research (NWO) funding.

Appendix: Intercalibration of Fish Canyon Tuff and Drachenfels $^{40}\text{Ar}/^{39}\text{Ar}$ standards for irradiation batch VU69-A

$^{40}\text{Ar}/^{39}\text{Ar}$ ages reported in this paper are calculated relative to the Vrije Universiteit Amsterdam in-house standard Drachenfels. The age for this standard was originally reported as 25.26 Ma relative to Taylor Creek Rhyolite sanidine of 27.92 Ma (Wijbrans et al. 1995). Recent updates of international standard ages require also an update for the age of Drachenfels sanidine. Drachenfels sanidine has been used as main flux monitor in irradiation batch VU69. Along with Drachenfels, the Fish Canyon Tuff sanidine standard has been loaded on several locations next to Drachenfels. Here we provide the intercalibration

data set between these two standards for irradiation batch VU69-A, the same batch in which the Glogovnica, Sjeniĉak and Paripovac samples are irradiated (Table 3). A compilation of Drachenfels—FC over a series of irradiations batches is in progress. $(^{40}\text{Ar}^*/^{39}\text{ArK})_{\text{Drachenfels}}/(^{40}\text{Ar}^*/^{39}\text{ArK})_{\text{Fish Canyon}}$ ratios (or R-values) are calculated for three pairs of Drachenfels—Fish Canyon Tuff standards (A1 and A2, A16 and A17 and A31 and A32; Table 2). In Table A1 (online supplementary material), all relevant analytical data are reported.

Weighted mean of R(A16-A17) and R(A32-A31) yields 0.9028 ± 0.0008 (Table 4). This yields in an age of 25.477 ± 0.030 Ma for Drachenfels relative to FCs of 28.198 ± 0.022 Ma of Kuiper et al. (2008) when using Steiger and Jäger (1977) decay constants. This translates to 25.479 ± 0.030 Ma for Drachenfels relative to FCs of 28.201 ± 0.022 Ma of Kuiper et al. (2008) when using Min et al. (2000) decay constants compilation. It is unclear why the data pair A1 and A2 is an outlier, although the

Table 3 Overview of relevant samples and standards in irradiation batch VU69A

Irradiation code	Sample code	Run code MAP215-50	Position in irradiation vial—height (in mm)
VU69-A1	Drachenfels	08j0002; 08j0042; 08j0053	0.5
VU69-A2	VN-FCT-98	08j0003	2.8
VU69-A6	Drachenfels	08j0004; 08j0044; 08j0056; 08j0188	12.6
VU69-A11	Drachenfels	08j0005; 08j0046; 08j0093; 08j0189	23.4
VU69-A14	Glogovnica	08m0048	30.1
VU69-A16	Drachenfels	08j0006; 08j0049; 08j0096	33.9
VU69-A17	VN-FCT-98	08j0007	35.9
VU69-A18	Sjeniĉak	08m0050	37.9
VU69-A21	Drachenfels	08j0008; 08j0051; 08j0058; 08j0098	42.9
VU69-A23	Paripovac	08m0059	46
VU69-A26	Drachenfels	08j0009; 08j0062; 08j0102; 08j0190	51.4
VU69-A31	VN-FCT-98	08j0010	56.6
VU69-A32	Drachenfels	08j0011; 08j0065	57.9

Table 4 R values of three Drachenfels/Fish Canyon Tuff pairs

Irradiation code	Standard	$^{40}\text{Ar}/^{39}\text{Ar}_K$	$\pm 1\sigma$	$\pm 1\sigma$ (%)	MSWD	N
VU69-A1	Dra-1	5.4878	± 0.0089	0.16	2.37	5
VU69-A2	VN-FCT-98	5.9932	± 0.0053	0.09	1.55	6
VU69-A16	Dra-1	5.3222	± 0.0054	0.10	2.02	9
VU69-A17	VN-FCT-98	5.8979	± 0.0084	0.14	1.08	7
VU69-A32	Dra-1	5.4755	± 0.0042	0.08	1.51	9
VU69-A31	VN-FCT-98	6.0644	± 0.0041	0.07	0.94	7
R						$\pm 1\sigma$
R _{A2} ^{A1}		0.9157				0.0017
R _{A17} ^{A16}		0.9024				0.0016
R _{A31} ^{A32}		0.9029				0.0009

individual analyses of A1 and to a lesser extent A2 are very heterogeneous.

References

- Altherr R, Lugović B, Meyer H-P, Majer V (1995) Early Miocene post-collisional calc-alkaline magmatism along the easternmost segment of the Periadriatic fault system (Slovenia and Croatia). *Miner Petrol* 54:225–247
- Aničić B, Ogorelec B, Kralj P, Mišić M (2002) Litološke značilnosti terciarnih plasti na Kozjanskem. (Lithology of Tertiary beds in Kozjansko, Eastern Slovenia). *Geologija* 45:213–246
- Avanić R, Pécskay Z, Wacha L, Palinkaš L (2005) K–Ar dating of glauconitic sediments in Macelj Mt. (NW Croatia). In: Velić I, Vlahović I, Biondić R (eds) *Knjiga sažetaka, 3. Hrvatski geološki kongres. Hrvatski geološki institut, Zagreb*, pp 5–6
- Bennet RA, Hreinsdottir S, Buble G, Bašić T, Bačić Z, Marjanović M, Casale G, Gendaszek A, Cowan D (2008) Eocene to present subduction of southern Adria mantle lithosphere beneath the Dinarides. *Geology* 36:3–6
- Bulić J, Jurišić-Polšak Z (2009) The lacustrine Miocene deposits at Crnika beach on the island of Pag (Croatia). *Geol Croatica* 62:135–156
- Ćorić S, Pavelić D, Rögl F, Mandić O, Vrabac S, Avanić R, Jerković L, Vranjković A (2009) Revised Middle Miocene datum for initial marine flooding of North Croatian Basins (Pannonian Basin System, Central Paratethys). *Geol Croatica* 62:31–43
- Csepregyhnyé Meznerics I (1967) Az Ipolytarnoci Burdigalai fauna. *Földtani Közlöny* 97:177–185
- De Leeuw A, Mandić O, Vranjković A, Pavelić D, Harzhauser M, Krijgsman W, Kuiper KF (2010) Chronology and integrated stratigraphy of the Miocene Sinj Basin (Dinaride Lake System, Croatia). *Palaeogeogr Palaeoclimatol Palaeoecol* 292:155–167
- Dolton GL (2006) Pannonian Basin Province, Central Europe (Province 4808). *Petroleum geology, total petroleum systems, and petroleum resource assessment. USGS Bull* 2204-B:1–47
- Fodor L, Csontos L, Bada G, Györfi I, Benkovics L (1999) Tertiary tectonic evolution of the Pannonian basin system and neighbouring orogens: a new synthesis of palaeostress data. In: Durand B, Jolivet L, Horvath F, Seranne M. (eds) *The Mediterranean Basins: tertiary extension within the Alpine Orogen. Geol Soc Spec Publ* 156:295–334
- Fodor L, Jelen B, Márton E, Rifelj H, Kraljić M, Kevrić R, Márton P, Koroknai B, Báldi-Beke M (2002) Miocene to Quaternary deformation, stratigraphy and paleogeography in Northeastern Slovenia and Southwestern Hungary. *Geologija* 45(1):103–114
- Hajek-Tadesse V, Belak M, Sremac J, Vrsaljko D, Wacha L (2009) Early Miocene ostracods from the Sadovi n (Mt. Požeška gora, Croatia). *Geol Carpathica* 60:251–261
- Hamor G (1970) The Miocene of the East Mecsek Mts (in Hungarian). *Ann Inst Geol Hung* 53:1–483
- Hámor G (ed) (1988) *Neogene palaeographic atlas of Central and Eastern Europe. Hungarian Geological Institute*
- Harzhauser M, Mandić O (2008) Neogene lake systems of Central and South-Eastern Europe: faunal diversity, gradients and interrelations. *Palaeogeogr Palaeoclimatol Palaeoecol* 260:417–434
- Harzhauser M, Piller WE (2007) Benchmark data of a changing sea. *Palaeogeography, palaeobiogeography and events in the Central Paratethys during the Miocene. Palaeogeogr Palaeoclimatol Palaeoecol* 253:8–31
- Hölzel M, Wägrich M (2004) Sedimentology of a Miocene delta complex: the type section of the ingering formation (Fohnsdorf Basin, Austria). *Austrian J Earth Sci* 95–96:80–86
- Horvath F, Tari G (1999) IBS Pannonian Basin project: a review of the main results and their bearings on hydrocarbon exploration. In: Durand B, Jolivet L, Horvath F, Seranne M. (eds) *The Mediterranean Basins: Tertiary Extension within the Alpine Orogen. Geol Soc Spec Publ* 156:195–213
- Hohenegger J, Rögl F, Ćorić S, Pervesler P, Lirer F, Roetzel R, Scholger R, Stingl K (2009) The Styrian Basin: a key to the Middle Miocene (Badenian/Langhian) Central Paratethys transgressions. *Austrian J Earth Sci* 102:102–132
- Hrvatović H (2006) *Geological guidebook through Bosnia and Herzegovina. Geological Survey of Federation BiH, Sarajevo*
- Jelen B, Rifelj H (2003) The Karpatian in Slovenia. In: Brzobohatý R, Cicha I, Kováč M, Rögl F (eds) *The Karpatian. Masaryk University, Brno*, pp 133–139
- Jurković I (1993) Mineraline sirovine sisačkog područja. *Rudarsko-geološko-naftni zbornik* 5:39–58
- Knežević S (1996) New *Congerina* from Šumadija and Pomoravlje. In: Krstić N (ed), *Neogene of Central Serbia. Spec Publ Geoinstitute* 19:27–31
- Kochansky-Devidé V, Slišković T (1978) Miocenske kongerije Hrvatske, Bosne i Hercegovine. *Palaeont Jugoslavica* 19: 1–98
- Kóky J (2006) Nonmarine mollusc fauna from the Lower and Middle Miocene, Bakony Mts, W Hungary. *Geol Hungarica Ser Palaeont* 56:1–196
- Konečný V, Kováč M, Lexa J, Šefara J (2002) Neogene evolution of the Carpatho-Pannonian region: an interplay of subduction and back-arc diapiric uprising in the mantle. *EGU Stephan Mueller Spec Publ Ser* 1:105–123
- Koppers AAP (2002) ArArCALC—software for $^{40}\text{Ar}/^{39}\text{Ar}$ age calculations. *Comput Geosci* 28:605–619
- Kovács I, Csontos L, Szabó C, Bali E, Falus G, Benedek K, Zajacz Z (2007) Paleogene–early Miocene igneous rocks and geodynamics of the Alpine-Carpathian-Pannonian-Dinaric region: an integrated approach. *Geol Soc Am Spec Pap* 418:93–112
- Krizmanić K (1995) Palynology of the Miocene bentonite from Gornja Jelenska (Mt. Moslavačka Gora, Croatia). *Geol Croatica* 48:147–154
- Krstić N, Savić L, Jovanović G, Bodor E (2003) Lower Miocene lakes of the Balkan Land. *Acta Geol Hungarica* 46:291–299
- Kuiper KF, Deino A, Hilgen FJ, Krijgsman W, Renne PR, Wijbrans JR (2008) Synchronizing rock clocks of Earth history. *Science* 320:500
- Lourens L, Hilgen F, Shackleton NJ, Laskar J, Wilson D (2004) The Neogene Period. In: Gradstein FM, Ogg JG, Smith AG (eds) *A Geologic Time Scale 2004. Cambridge University Press, Cambridge*, pp 409–440
- Lučić D, Saftić B, Krizmanić K, Prelogović E, Britvić V, Mesić I, Tadej J (2001) The Neogene evolution and hydrocarbon potential of the Pannonian Basin in Croatia. *Mar Petrol Geol* 18:133–147
- Mandić O, Ćorić S (2007) Eine neue Molluskenfauna aus dem oberen Otnangium von Rassing (NÖ)—taxonomische, biostratigraphische, paläoökologische und paläobiogeographische Auswertung. *Jahrb Geol Bundesanstalt* 147:387–398
- Mandić O, Pavelić D, Harzhauser M, Zupanić J, Reischenbacher D, Sachsenhofer RF, Tadej N, Vranjković A (2009) Depositional history of the Miocene Lake Sinj (Dinaride Lake System, Croatia): a long-lived hard-water lake in a pull-apart tectonic setting. *J Paleolimnol* 41:431–452
- Milojević R (1976) Mineralne sirovine Bosne i Hercegovine. Prvi tom, Ležišta uglja. Ležišta nemetala. *Geoinžinjeri, Sarajevo*
- Min KW, Mundil R, Renne PR, Ludwig KR (2000) A test for systematic errors in $^{40}\text{Ar}/^{39}\text{Ar}$ geochronology through comparison with U/Pb analysis of a 1.1-Ga rhyolite. *Geochim Cosmochim Acta* 64(1):73–98

- Mutić R (1979) Tufovi u donjohelvetskim naslagama u području Brestika i Bojne (Banija, Hrvatska). *Geol Vjesnik* 31:253–266
- Ožegović F (1944) Prilog geologiji mlađeg terciara na temelju podataka iz novijih dubokih bušotina u Hrvatskoj. *Vjestnik Hrvatskog Državnog Geol Zavoda* 2:391–491
- Palfy J, Mundil R, Renne PR, Bernor RL, Kordos L, Gasparik M (2007) U–Pb and $^{40}\text{Ar}/^{39}\text{Ar}$ dating of the Miocene fossil track site at Ipolytarnóc (Hungary) and its implications. *Earth Planet Sc Lett* 258:160–174
- Pamić J, Gušić I, Jelaska V (1998) Geodynamic evolution of the Central Dinarides. *Tectonophysics* 297:251–268
- Pavelić D (2001) Tectonostratigraphic model for the North Croatian and North Bosnian sector of the Miocene Pannonian Basin System. *Basin Res* 13:359–376
- Pavelić D, Kovačić M (1999) Lower Miocene alluvial deposits of the Požeška Mt. (Pannonian Basin, Northern Croatia): cycles, megacycles and tectonic implications. *Geol Croatica* 52: 67–76
- Pavelić D, Miknić M, Sarkotić Šlat M (1998) Early to Middle Miocene facies succession in lacustrine and marine environments on the southwestern margin of the Pannonian basin system. *Geol Carpathica* 49:433–443
- Pavelić D, Avanić R, Bakrač K, Vrsaljko D (2001) Early Miocene Braided river and Lacustrine sedimentation in the Kalnik mountain area (Pannonian Basin System, NW Croatia). *Geol Carpathica* 52:375–386
- Pavelić D, Avanić R, Kovačić M, Vrsaljko D, Miknić M (2003) An outline of the evolution of the Croatian part of the Pannonian Basin System. In: Vlahović I, Tišljarić J (eds) Evolution of depositional environments from the Palaeozoic to the quaternary in the Karst Dinarides and the Pannonian Basin. 22nd IAS meeting of sedimentology. Field Trip Guidebook. Institute of Geology, Zagreb, pp 155–161
- Petrović M, Atanacković M (1969) Biostratigrafska analiza foraminifera tortonskog kata severoistočnog Potkozarja. *Geol Glasnik* 13:141–158
- Petrović M, Atanacković M (1976) Biostratigrafija tortonskog kata severnog Podkozarja i okoline sela Hrvacani na osnovu foraminifera (severozapadna Bosna). *Geol Anali Balkanskog Poluostrva* 40:65–101
- Piller WE, Harzhauser M, Mandić O (2007) Miocene Central Paratethys stratigraphy—current status and future directions. *Stratigraphy* 4:151–168
- Placer L (2008) Principles of the tectonic subdivision of Slovenia. *Geologija* 51(2):205–217
- Pletikapić Z (1960) Građa Savske potoline na području između Zrinske i Moslavačke gore. *Geol Vjesnik* 13:121–130
- Poljak J (1942) Prilog poznavanju geologije Kalničke gore. *Vjestnik Hrvatskog Državnog Geol Zavoda* 1:53–103
- Popov SV, Rögl F, Rozanov AY, Steininger FF, Shcherba IG, Kováč M (2004) Lithological-Paleogeographic maps of Paratethys. 10 maps late Eocene to Pliocene. *Courier Forschungsinstitut Senckenberg* 250:1–46
- Prelogović E (1975) Neotektonska karta SR Hrvatske. *Geol Vjesnik* 28:97–108
- Rasser MW, Harzhauser M, Anistratenko O, Anistratenko VV, Bassi D, Belak M, Berger J-P, Bianchini G, Čičić S, Čosović V, Doláková N, Drobne K, Filipescu S, Gürs K, Hladilová Š, Hrvatović H, Jelen B, Kasinski JR, Kovač M, Kralj P, Marjanac T, Márton E, Mietto P, Moro A, Nagymarosy A, Nebelsick JH, Nehyba S, Ogorelec B, Oszczypko N, Pavelić D, Pavlovec R, Pavšič J, Petrová P, Piwocki M, Poljak M, Pugliese N, Redžepović R, Rifelj H, Roetzel R, Skaberne D, Sliva L, Standke G, Tunis G, Vass D, Wagreich M, Wesselingh F (2008) Paleogene and Neogene of Central Europe. In: McCann T (ed) *The Geology of Central Europe, vol 2: mesozoic and cenozoic*. Geological Society, London, pp 1031–1140
- Rögl F (1998) Paleogeographic considerations for Mediterranean and Paratethys seaways (Oligocene to Miocene). *Ann Naturhist Mus Wien, Serie A* 99:279–310
- Rögl F, Steininger F (1983) Vom Zerfall der Tethys zu Mediterran und Paratethys. *Ann Naturhist Mus Wien* 85A:135–163
- Sachsenhofer RF, Jelen B, Hasenhüttl C, Dunkl I, Rainer T (2001) Thermal history of Tertiary basins in Slovenia (Alpine-Dinaride-Pannonian junction). *Tectonophysics* 334:77–99
- Saftić B, Velić J, Sztanó O, Juhász G, Ivković Ž (2003) Tertiary subsurface facies, source rocks and hydrocarbon reservoirs in the SW part of the Pannonian Basin (Northern Croatia and South-Western Hungary). *Geol Croatica* 56:101–122
- Schmid SM, Bernoulli D, Fügenschuh B, Matenco L, Schefer S, Schuster R, Tischler M, Ustaszewski K (2008) The Alpine-Carpathian-Dinaridic orogenic system: correlation and evolution of tectonic units. *Swiss J Geosci* 101:139–183
- Schultz O (2003) *Bivalvia neogenica (Lucinoidea-Mactroidea)*. In: Piller WE (ed) *Catalogus Fossilium Austriae, Band 1/Teil 2*. Verlag der Österreichischen Akademie der Wissenschaften, Wien, pp 381–690
- Šikić L, Jović B (1968) Starost “Gornjooligocenskih” naslaga sa sredim ugljenom u području Pregrade (sjeverna Hrvatska). *Geol Vjesnik* 22:333–346
- Šimunić A, Pamić J (1993) Geology and petrology of Egerian-Eggenburgian andesites from the easternmost parts of the Pannonic zone in Hrvatsko Zagorje (Croatia). *Acta Geol Hungarica* 36:315–330
- Šimunić A, Avanić R, Šimunić A (1990) “Maceljski pješčenjaci” i vulkanizam zapadnog dijela Hrvatskog zagorja (Hrvatska, Jugoslavija). *Rad JAZU* 449:179–194
- Steiger RH, Jäger E (1977) Subcommission on geochronology: convention on the use of decay constants in geo- and cosmochronology. *Earth Planet Sc Lett* 36:359–362
- Strauss P, Harzhauser M, Hinsch R, Wagreich M (2006) Sequence stratigraphy in a classic pull-apart basin (Neogene, Vienna Basin). A 3D seismic based integrated approach. *Geol Carpathica* 57:185–197
- Tari V (2002) Evolution of the northern and western Dinarides: a tectonostratigraphic approach. *EGU Stephan Mueller Spec Publ Ser* 1:223–236
- Tari V, Pamić J (1998) Geodynamic evolution of the northern Dinarides and the southern part of the Pannonian Basin. *Tectonophysics* 297:269–281
- Tibljaš D, Loparić V, Belak M (2002) Discriminant function analysis of Miocene volcanoclastic rocks from North-Western Croatia based on geochemical data. *Geol Croatica* 55:39–44
- Tomljenović B, Csontos L (2001) Neogene–Quaternary structures in the border zone between Alps, Dinarides and Pannonian Basin (Hrvatsko zagorje and Karlovac Basins, Croatia). *Int J Earth Sci* 90:560–578
- Tomljenović B, Csontos L, Márton E, Márton P (2008) Tectonic evolution of the northwestern Internal Dinarides as constrained by structures and rotation of Medvednica Mountains, North Croatia. In: Siegesmund S, Fügenschuh B, Froitzheim N (eds) *Tectonic Aspects of the Alpine-Dinaride-Carpathian System*. *Geol Soc Spec Publ* 298:147–167
- Vrsaljko D, Pavelić D, Bajraktarević Z (2005) Stratigraphy and Palaeogeography of Miocene Deposits from the Marginal Area of Žumberak Mt. and the Samoborsko Gorje Mts. (Northwestern Croatia). *Geol Croatica* 58:133–150
- Wijbrans JR, Pringle MS, Koppers AAP, Scheveers R (1995) Argon geochronology of small samples using the Vulkan argon laserprobe. *Proc Kon Ned Akad v Wetensch* 98:185–218
- Zachos J, Pagani M, Sloan S, Thomas E, Billups K (2001) Trends, rhythms, and aberrations in global climate 65 Ma to present. *Science* 292:686–693